Nonlinear control of the optical delay line pathlength

Boris J. Lurie, John J. Hench, Asif Ahmed, Fred Y. Hadaegh

Jet Propulsion Laboratory, California Institute of Technology
4800 Oak Grove Drive, Pasadena, CA 91109

ABSTRACT

This paper discusses the problem of designing a control system for an interferometer delay line which contains coarse-vernier loops. The vernier loop compensator has nonlinear dynamics and includes a local feedback path containing a deadzone. This accomplishes two objectives: global stability and good transient response to large signals. In addition, by ensuring global stability in the vernier loop, the gain of the coarse loop may be increased thus providing greater disturbance rejection in the overall loop.

Keywords: Nonlinear control, main-vernier control, optical delay line, interferometer

1. INTRODUCTION

An optical interferometer is a device which combines two beams of light gathered from widely separated optical elements called siderostats in such a way that the beams of light produce an interference pattern on the focal plane. In so doing, it is able to perform various astrometric measurements. The mechanism which ensures that the light pathlengths from the two sources are adjusted properly is the optical delay line.

For the space-based interferometer that will make up the Space Interferometer Mission (SIM) the delay line is positioned on a truss structure as shown in Figure 1. A reaction wheel assembly is employed for the interferometer attitude control. The delay line itself consists of two movable mirrors. The larger mirror is spherical. It is moved by a voice coil actuator (VC) capable of the maximum displacement of 1 cm at low frequencies. A smaller, flat mirror is moved by a piezoelectric actuator (PZT) with the maximum stroke 30 μm. The light bouncing between the mirrors is delayed by the combined stroke of the PZT and the VC actuators.

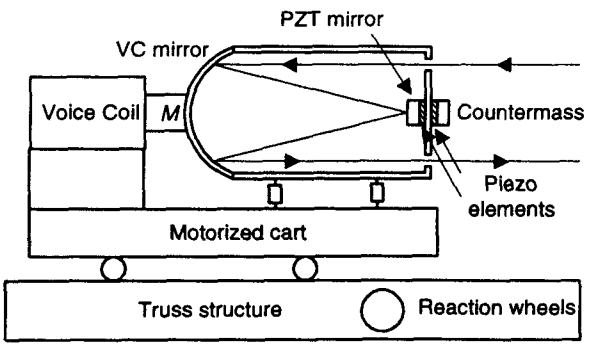

Figure 1 Optical delay line

The PZT consists of two piezoelectric elements and applies a force between the smaller mirror and a countermass. Since the forces applied to the supporting structure are balanced, the PZT does not excite the structure. Because the PZT loop is not affected by structural modes of the spherical mirror assembly; the feedback bandwidth in this loop can therefore be made wide, up to 1 kHz.

The control setup may be viewed as in terms of a coarse-vernier loop structure. The fine control is done by the PZT. The function of the VC is to de-saturate the PZT for commanded strokes larger than the saturation level of the PZT. The same coarse-vernier functionality exists between the VC and the motorized cart; however, this loop will not be discussed here.

* Correspondence: blurie@pop.jpl.nasa.gov; Telephone: (818)354-3690; Fax: (818)393-4440

The voice coil moves the mirror having mass $M = 0.5$ kg against the flexible structure with mobility Z_{st}. The equivalent electrical schematic diagram for the VC actuation of the mirror is shown in Figure 2. Here, C_M reflects the mass of the mirror. The VC output impedance is negligibly small.

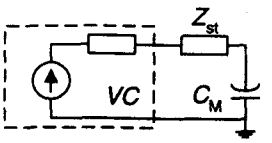

Figure 2 Equivalent electrical circuit for the voice coil and the mirror

2. NUMERICAL DESIGN CONSTRAINT

The PZT maximum displacement is $D_{pzt} = 0.00003$ m over the entire frequency range of interest. The VC maximum displacement amplitude is

$$D_{vc} = (2\pi f_{cross})^{-2} kI_{max}/M,$$

where $k = 0.3$ N/A is the VC constant, $I_{max} = 3$ A is the current saturation threshold of the VC driver amplifier, and where f_{cross} is the frequency at which the VC maximum displacement amplitude D_{vc} equals that of the PZT. Solving for f_{cross} we have

$$f_{orces} = [kI_{max}/(MD_{pzt})]^{1/2}/(2\pi) \approx 40 \text{ Hz}.$$

The feedback in the VC and PZT loops must be sufficiently large to reject the vibrational disturbances caused by the reaction wheels. These disturbances are significant up to 500 Hz. The feedback must be at least 60 dB at 16 Hz. The spectral density of the disturbance forces is assumed to be relatively flat over the 500 Hz bandwidth, so that the vibration amplitudes are, on the average, inversely proportional to the square of the frequency. Therefore, both the feedback and the maximum actuator output amplitude can decrease inversely proportional to the square of the frequency, i.e., the loop gain slope can be –12 dB/octave. In accordance with the feedback area preservation principles described by the Bode integrals [1,2,3], the loop gain slope should be close to –12 dB/octave.

The available feedback in the VC loop is constrained by the uncertain mobility of the structure Z_{st}. This may be estimated using an asymptotic Bode-step response. If the loop is designed as stand-alone-stable, the structural modes and their uncertainties prevent the VC loop bandwidth to exceed 100 Hz. In this case the gain in the VC loop at 16 Hz is only 26 dB, less than the required 60 dB.

Therefore, the VC loop has to be designed as stand-alone-unstable; this allows the gain and the slope of the loop shape in Bode diagram to be substantially increased.

The sampling frequency is 5 kHz for the PZT loop and 1 kHz for the VC loop.

3. HIGHER-LEVEL DESIGN OBJECTIVES

The control system performance index is the mean square error in the delay line pathlength. The principle design objective is to keep the mean square error below 5 nm.

In addition to the principle design objective, the following characteristics are required or highly desirable:

- system robustness,
- good output responses to commands of different shapes and amplitudes,
- transient responses to large amplitude vanishing disturbances that neither excessive large in amplitude nor duration (In general, nonlinear phenomena responses can be prolonged and violent.), and,
- large disturbance/command triggering threshold of these nonlinear phenomena, in order that these nonlinear phenomena happen infrequently.

4. DESIGN APPROACH

The controller for this nonlinear, flexible, and uncertain plant must be reasonably close to the best achievable, but not overly complicated. We choose the controller to be multiloop, high-order, and nonlinear, but not time varying (i.e. not adaptive).

The conceptual design employing Bode integrals and the Bode asymptotic diagrams should produce a controller which best satisfies the higher-level design objectives.

The design begins with making some reasonable assumptions and translating the higher-level objectives into a set of lower-level guidelines. The latter consists of design objectives and design considerations. If possible, these objectives and considerations should be formulated in a mutually decoupled (orthogonal) form to simplify the system trade-offs and to speed up the design process. This is more easily accomplished using frequency-domain specifications.

5. LOWER LEVEL DESIGN OBJECTIVES

The lower level design objectives for the feedback system under consideration can be formulated as the following:

- To effectively reject the vibrational disturbances of rather large amplitudes, the VC loop gain must exceed 50 dB at 40 Hz and the feedback must increase toward the lower frequencies.
- To effectively reject vibrations at higher frequencies, however with smaller amplitudes, the feedback in PZT loop must have wide bandwidth; 600 Hz bandwidth will suffice.
- The quality of the transient response should be relatively insensitive to step commands of different amplitudes.
- The system must be globally stable.
- If the VC loop is made unstable when stand-alone, the frequency of oscillation in this loop should be as high as possible for the amplitude of the limit-cycle oscillation in this loop to be correspondingly small thereby not overloading the PZT actuator.

6. THE DESIGN CONSIDERATIONS

- The VC and PZT loops are nearly minimum phase, and the combined loop must be minimum phase. For this, the parallel channels' responses must be shaped appropriately.
- At frequencies below $f_{cross} \approx 40$ Hz the VC provides a larger stroke and is therefore the main actuator; at higher frequencies, PZT is the main actuator. Therefore, rejection of the maximum amplitude disturbances depends at $f < f_{cross}$ on the loop gain in VC loop and at $f > f_{cross}$, on the PZT loop. Outside of these ranges, the only requirements for the VC and PZT loop gain shaping is the provision of stability and robustness.
  (Generally, making the loop to cross at f_{cross} is not necessary. Extra gain in the loop which is not the main one does not hurt the system performance – but it unnecessarily consumes a part of the area specified by a related Bode integral.)
- At the frequency of 5 Hz, the VC driver output impedance should be small to damp the VC main suspension resonance, or else the feedback at this frequency will be unnecessarily large. This is not desirable in view of the trade-offs described by the Bode integrals. At frequencies over 50 Hz, the impedance can be made higher in order for the loop transfer function at these frequencies to be less affected by the system structural modes.

7. CONVENTIONAL DESIGN APPROACH

In general, industrial coarse-vernier system do not include nonlinear dynamic compensators (NDCs) or only include simple NDCs for improving the responses to the commands. Such systems are made globally stable by making all stand-alone loops globally stable [4].

When the feedback and the disturbance rejection in such systems are not sufficient, the disturbance rejection can be improved at the price of making the coarse-vernier system as only conditionally stable [5,6]. This causes however the command generator to be complicated and the reaction to the commands sluggish. It also necessitates a procedure to recover the system from the limit cycle which can be quite violent and damaging for the hardware. For this reason this option is normally not used in industrial systems.

8. CHOSEN DESIGN OPTIONS

The chosen design options for the system with an NDC are the following:

- The VC loop is stand-alone-unstable. In this case the slope of the Bode diagram of the VC loop can be made steeper thus improving the disturbance rejection and the handling of large amplitude disturbances.
- An NDC provides global stability.
- PZT loop bandwidth is 600 Hz wide, with Bode step response, with the Bode diagram slope −10 dB/oct at frequencies 150 to 1200 Hz, and −12 dB/oct over the range 40 to 150 Hz. At 40 Hz the gain in the PZT loop is therefore 12 dB/octave × $\log_2(150/40)$ + 20 = 43 dB. The gain may gradually roll down at lower frequencies.
- We choose the asymptotic Bode diagrams shown in Figure 3(a), since for this particular design task the advantages of

using the better shaped diagrams [2,3] exemplified in (b) do not justify higher complexity of the design.

- The VC loop Bode diagram crosses the PZT loop Bode diagram at 40 Hz.
- The PZT lag at 40 Hz is approximately 140°.
- The VC loop Bode diagram slope is −18 dB/oct down to 20 rad/sec, and −6 dB/oct below this frequency. The gain at 40 Hz must be 43 dB i.e. 141 times. From here, $T_{VC} = a/[s(s+20)^2]$ where $a = 141(2\pi 40)^3 = 2.24\times10^9$.
- At 40 Hz, the phase difference between the loops is 270 − 180 = 130°, resulting in 60° safety margin in guaranteeing the minimum phase characteristic of the total loop.
- To ensure global stability of the system and good transient responses to the commands, an NDC will be included in the combined loop, with the dead zone equal to the threshold of the PZT actuator. As the linear block of the NDC, the PZT loop transfer function is employed.

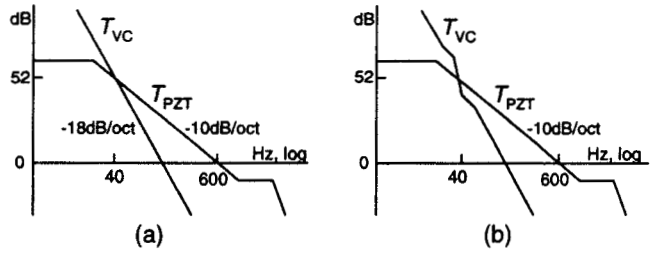

Figure 3 Asymptotic Bode diagrams for stand-alone loop transfer functions; (a) simpler and (b) higher performance

9. BLOCK DIAGRAM WITH RATIONAL FUNCTIONS

The asymptotic (transcendental) responses shown in Figure 3(a) need to be approximated with rational function responses.

The frequency-normalized Bode-step-type loop response (including certain nonminimum phase lag due to sampling) is obtained with MATLAB function `bostep` (from the Bode Step toolbox in [3]) and shifted in frequency with `lp2lp` for the crossover frequency to be $2\pi600$ rad/sec. This forms the stand-alone PZT loop transfer function. The stand-alone VC loop transfer function has been already defined.

The Bode and Nyquist diagrams shown in Figure 4 indicate that the system in the linear mode of operation is stable, robust, and provides 69 dB disturbance rejection at 16 Hz.

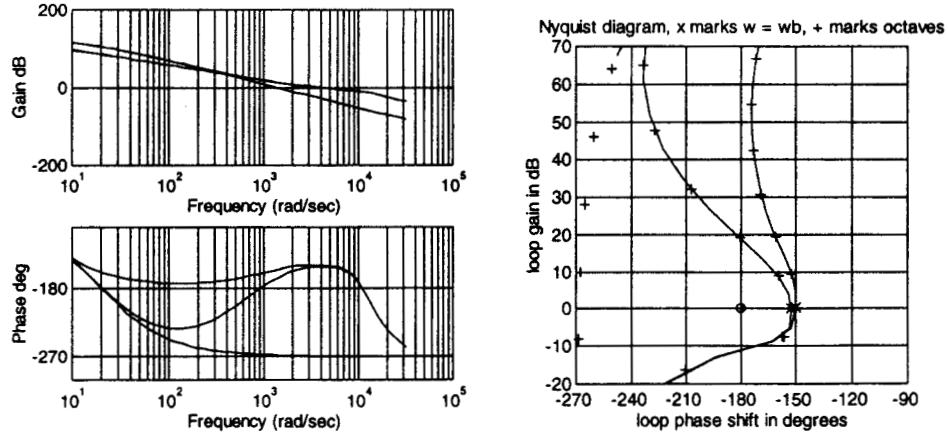

Figure 4 Bode and Nyquist diagrams for the rational transfer function approximating the asymptotic diagrams for the VC, the PZT, and the combined loop. (The combined response is the top one on the gain response, and the intermediate one among the phase responses and the Nyquist diagrams)

The SIMULINK block diagram using these transfer functions is shown in Figure 5. The controlled variable pathlength is the sum of the displacements produced by the PZT and VC actuators.

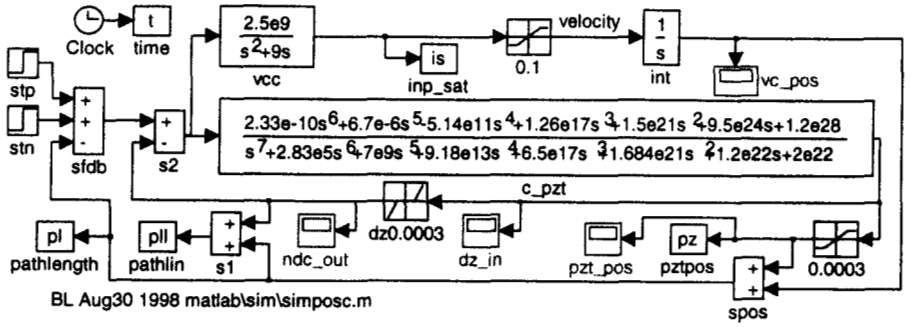

Figure 5 Simplified SIMULINK block diagram of pathlength control

In this block diagram and in the simulations, the thresholds of the saturation, the dead zone, and the signals amplitudes have been increased 10 times relative to the real system. This increases the numerical stability of simulation; the presence of the dead zones and the saturators makes the differential equations extremely stiff. This scaling, certainly, does not affect the theory of operation and the responses' shapes.

To simplify the analysis, VC is represented by a velocity source with velocity saturation; using a detailed VC actuator model should not change the principle character of the results.

The feedback path via the dead zone (dz0.0003 in Figure 5) implements nonlinear dynamic compensation (NDC). The dead zone equals the PZT saturation threshold. It does not pass small amplitude signals and has no effect on the system performance in the linear state of operation. The beneficial effect of the NDC on the global stability and the transient responses to large amplitude commands will be discussed later.

10. SELF-OSCILLATION IN A SYSTEM WITHOUT NONLINEAR DYNAMIC COMPENSATION

With frequency responses shown in Figure 4, the system is stable in the linear mode of operation when both the PZT loop and the VC loop are closed. The stand-alone VC loop is unstable.

Without an NDC, the system is not globally stable. Figure 6 shows the pathlength oscillation triggered by 30msec, 3mm pulse command. The oscillation approaches a limit cycle with the period longer than 5 sec.

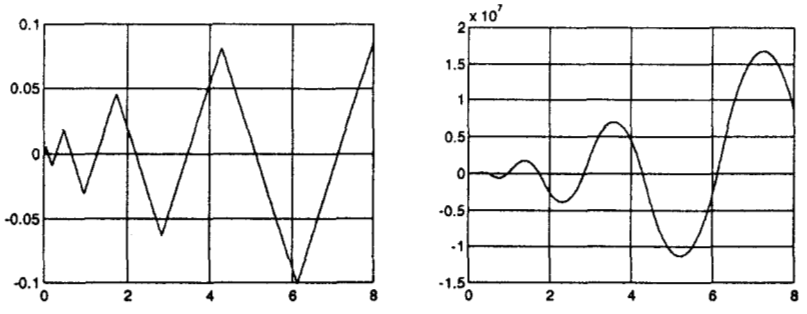

Figure 6: Oscillation triggered by a short pulse command in the system without an NDC, (a) of the VC output pathlength component and (b) at the input to saturation link

Compared to the amplitude of this oscillation, the PZT output is negligibly small. Therefore, the system can be analyzed as having a single nonlinear link, the saturation in the VC actuator, and the analysis can be performed with the describing function method. The accuracy of such analysis is sufficient since the VC loop is equivalent to a low-pass filter and the signal at the input to the saturation link becomes nearly sinusoidal when approaching the limit cycle as seen in Figure 6(b).

In other words, when the vibrations' amplitudes are large enough to saturate the PZT, the VC loop is left alone and the system bursts into the limit cycle self-oscillation at low frequency with large signal amplitude. When the high-amplitude high-frequency vibrations vanish and no longer saturate the PZT, the limit cycle oscillation does not change substantially since the amplitude of the output of the PZT is negligibly small compared to the displacement generated by the VC. Thus, the limit

cycle of the stand-alone VC loop is in fact also the limit cycle of the system as a whole. Large amplitude vanishing signals with substantial frequency components of the limit cycle oscillation belong to the basin of attraction for the limit cycle. The system is therefore conditionally stable.

11. LIMIT CYCLE OF THE VOICE COIL LOOP WITH THE NONLINEAR DYNAMIC COMPENSATOR

Since the stand-alone VC loop is unstable and the NDC dead zone does not pass the signals of small amplitudes, the stand-alone VC loop is unstable even with the NDC. It is important to emphasize, however, that the NDC radically changes the amplitude and the frequency of the limit cycle oscillation.

The amplitude of the limit cycle oscillation is determined by the dead zone in the NDC, since for signals much larger than the dead zone, the dead zone describing function approaches 1. In this case, the system becomes approximately linear, and such a system, as has been previously shown, is stable with sufficient stability margins. Therefore, the oscillation can only take place with amplitudes that are not significantly larger than the dead zone.

Since the oscillation amplitude is small, the describing function stability analysis indicates that the saturation link in the VC actuator can be replaced by a unity link, as shown in Figure 7(a). This systems' linear part is, however, unstable; for the conventional describing function methods to be applicable, the diagram (a) is transformed equivalently to the diagram (b) by replacing the dead zone with parallel connection of a unity link and a saturation link with the threshold equal to the dead zone. The stand-alone linear part of the latter (the dashed box) is stable since this is a feedback system with parallel connection of VC and PZT loops. The transfer function of the box is

$$\frac{T_{PZT}}{1+T_{VC}+T_{PZT}}.$$

Notice that the signal about the loop via the saturation is applied in phase.

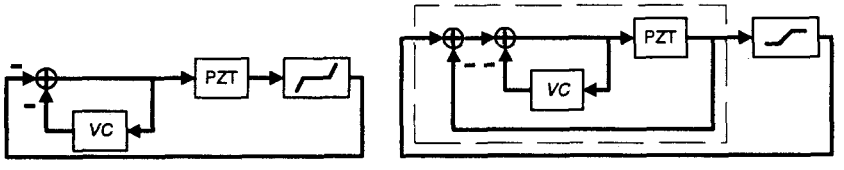

(a) (b)

Figure 7 Equivalent block diagrams for describing function analysis, (a) with the unstable linear part and (b) with the stable linear part

The Bode diagram for this transfer function is shown in Figure 8.

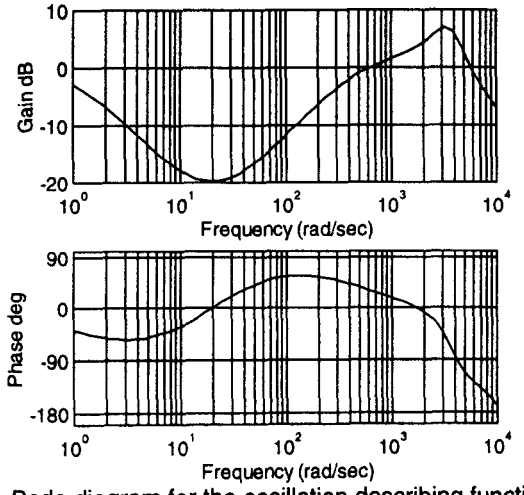

Figure 8 Bode diagram for the oscillation describing function analysis

The condition of oscillation (zero loop phase shift while the loop gain is positive) occurs at approximately 1600 rad/sec, or, approximately, at 250 Hz. The loop gain at this frequency is 3.5 dB, i.e. the gain coefficient is 1.5. The oscillation amplitude E can be found by equating the describing function to the inverse of the loop gain coefficient, i.e., using the approximate expression for the describing function from [2,3],

$$1.27(E/e_S)^{-1} - 0.27(E/e_S)^{-4} \approx 1/1.5,$$

from which $E \approx 1.8e_S \approx 0.00054$.

With this value of E, the describing function of the PZT equals 0.67, i.e. is only 3.5 dB less than the gain in the linear state of operation. Since in the linear state of operation the stability and safety margins of order of 10 dB are provided, the system is asymptotically globally stable.

Therefore, when the PZT actuator recovers from being saturated by disturbances or commands, it is capable of delivering the output signal comparable with the self-oscillation in the VC loop. Application of this signal makes the system stable, and the oscillation in the VC asymptotically dies down.

The time-history of the pathlength in this case is shown in Figure 9, (a) without and (b) with saturation in the VC that limits the slew rate.

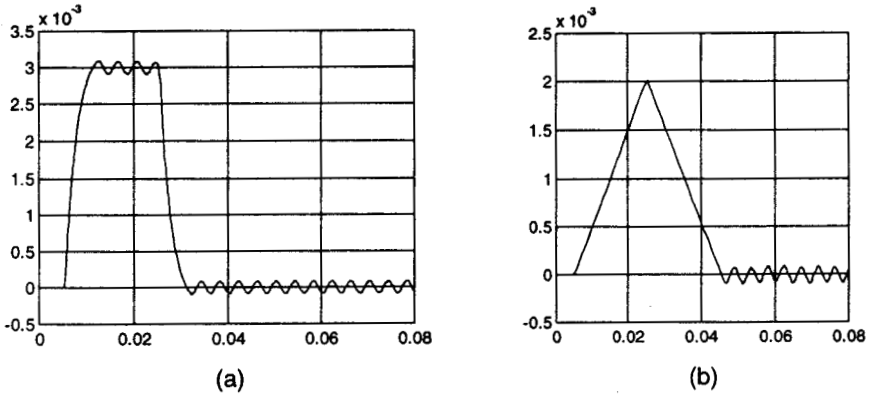

Figure 9 Pathlength time-history after a pulse command in a system with the NDC and without PZT actuator, (a) without limiting the VC velocity and (b) with ±0.1 m/sec limiter of the VC velocity

12. GLOBAL STABILITY OF A SYSTEM WITH THE NONLINEAR DYNAMIC COMPENSATOR

The dead-zone branch is in parallel with the PZT saturation branch. These two parallel branches are equivalent to a linear branch with the same transfer function. The system therefore includes only one nonlinear link: the VC saturation. The transfer function of the equivalent linear link from the VC saturation output to the VC saturation input is $T_{VC}/(1 + T_{PZT})$. The Bode diagram of this transfer function is plotted in Figure 10. Application of the Popov criterion [2,3] to this system shows that the system is asymptotically globally stable.

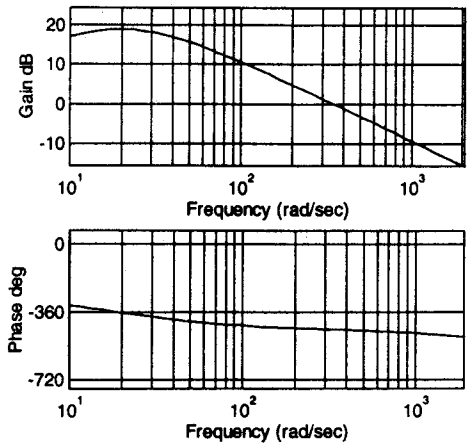

Figure 10 Bode diagram for transfer function $T_{VC}/(1 + T_{PZT})$.

13. TRANSIENT RESPONSES TO COMMANDS

The output transient response to a 3 mm pulse command in a system assuming no saturation in the VC actuator is shown in Figure 11.

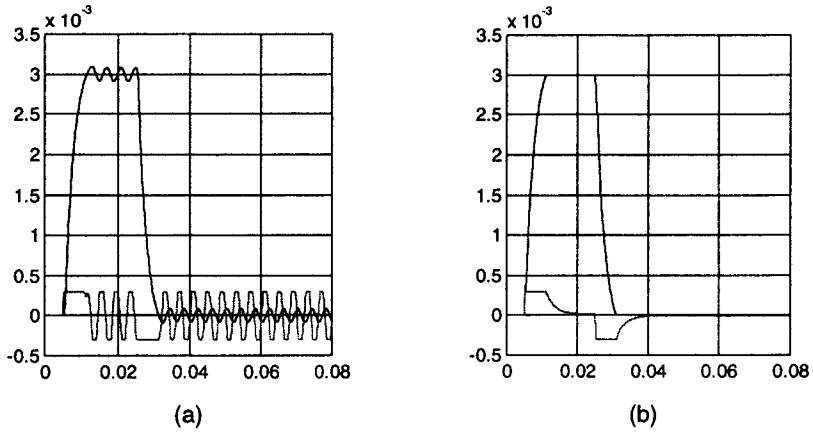

Figure 11 Closed-loop transient responses to 20 ms, 3 mm pulse command; pathlength, solid lines, and PZT mirror displacement time-response, dashed lines;
(a) without PZT, ending in a small-amplitude 250 Hz limit cycle oscillation, and
(b) with PZT, asymptotically globally stable, rapidly settling

Parts of the responses above are shown in more detail in Figure 12. After the PZT becomes desaturated, the NDC dead zone stops passing the signal, the pathlength response coincides with the response of the equivalent linear system, and the error dies down rapidly.

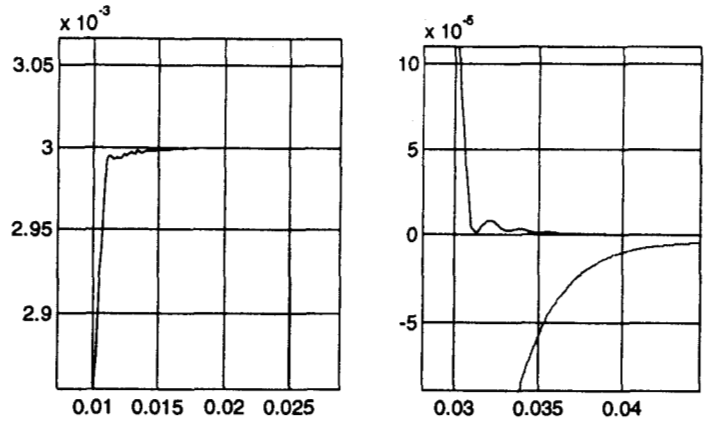

Figure 12 Detail of the closed-loop transient response to 20 ms, 3 mm pulse command

The output transient response to 50 ms pulse command in a system with saturation in the VC actuator with threshold 0.01 is shown in Figure 13. The saturation limits the slew rate of the output, and in other aspects the responses are similar to those in Figure 11.

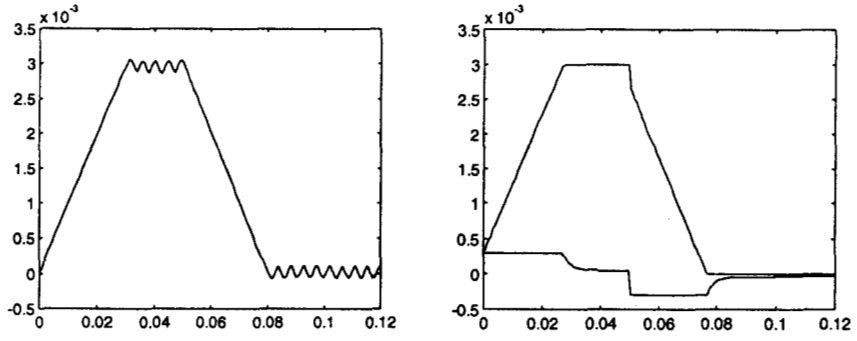

Figure 13 Closed-loop transient responses to 50 ms, 3 mm pulse command, with saturation in the VC actuator; pathlength, solid lines, and PZT mirror displacement time-response, dashed lines;
(a) without PZT, ending in a small-amplitude 250 Hz limit cycle oscillation, and
(b) with PZT, asymptotically globally stable, rapidly settling

Settling time to high accuracy is that of the linear system. The tail of the response is that of a linear system. Figure 14 shows the responses of the equivalent linear system (dotted line) and the response of the real system (solid line).

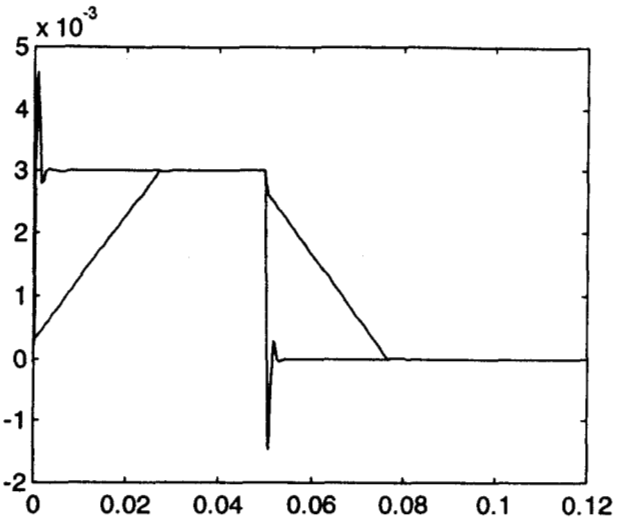

Figure 14 Transient responses to step commands, of the linear system (doted line) and the main-vernier nonlinear system (solid line)

These figures demonstrate the function of NDC: not only does it ensure global stability but also it provides good transient response to large signals.

In the large-signal (nonlinear) mode of operation, the loop response is, approximately, $T_{vc}/(1+T_{pzt})$. This loop response shown in Figure 10 is close to a single integrator response over the frequency range near the crossover, from 1 Hz to 15 Hz. Such loop response results in a single-pole closed loop transfer function which is known to produce a rather good closed-loop transient response (although not as good as a higher-order Bessel filter response, so there remains some room for improvement).

Figure 15 shows the output response to the (a) small and (b) large step commands applied at the instant of 50 msec. The 75% overshoot in the small-signal (linear) mode of operation results from the stability margins that are justifiably chosen reasonably narrow (since the plant parameter uncertainty is small). If needed, the small-signal overshoot can be reduced by a prefilter or command feedforward, but these are not needed because the overshoot is small in magnitude.

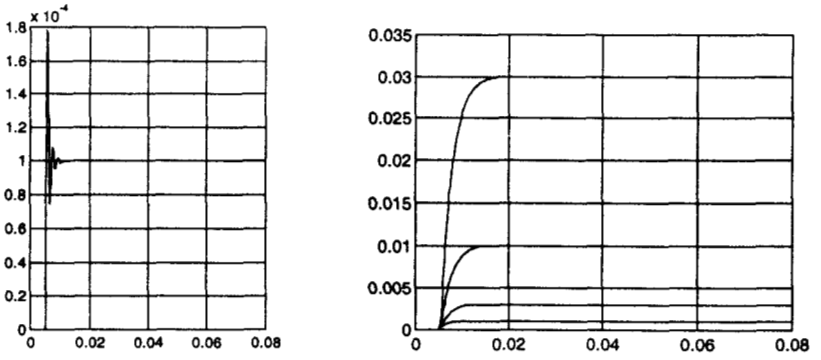

Figure 15 Transient responses to step commands of (a) 0.001 m and (b) larger amplitudes' commands

14. ROBUSTNESS

As long as the threshold in the PZT saturation is exactly equal to the dead zone in the NDC, the system is equivalent to a system with only one nonlinear element, VC actuator. This system satisfies the Popov criterion with conventional stability margins, and is therefore robust against variations in the linear links' transfer functions and in the nonlinear characteristic of the VC actuator.

Nevertheless, it would be desirable to make the dead zone wider than the threshold of the PZT saturation by 10 to 30% so as not to impair the PZT output stroke. Therefore, the system must be also robust against variations in the threshold of the saturation in the PZT. To such system including more than one nonlinear link, the Popov criterion is not applicable. The theoretical analysis can be made using some extensions of the Popov criterion based on the passivity approach [2,3], but we are not yet ready to present this material here. Instead, we rely on computer simulations. When the PZT saturation threshold is changed from 0.0003 to 0.00015, the system remains stable and the response to the pulse command shown in Figure 16 remains acceptable. Further reduction of the threshold to 0.0001 makes the system unstable and causes small amplitude oscillation similar to that shown in Figure 13.

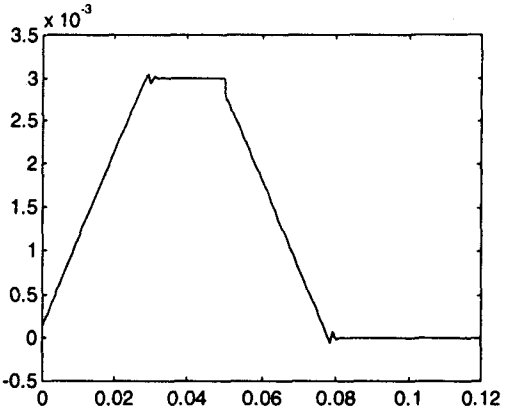

Figure 16 Transient responses to the pulse command in the system with PZT saturation threshold 0.00015

15. CONCLUSION

The coarse-vernier control system with the NDC is globally stable, with the disturbance rejection improved by an order of magnitude compared to the system without an NDC (which is not globally stable and has barely acceptable thresholds at which disturbances trigger a limit cycle). Furthermore, the responses to large commands have high slew rates and no overshoots.

The novel design method presented herein improves the coarse-vernier feedback system performance, compared to conventional control of the main-vernier actuator, in the following important aspects: it

- improves disturbance rejection, in the presented example by an order of magnitude
- provides global stability
- provides smooth transients to disturbances overloading the vernier actuator
- provides good transient response to the command, with negligible overshoot and small rise- and settling-times
- allows simplifying the commander by commanding only the destination point, i.e. using a step-function command and not a time-profiled command

The proposed approach is applicable to various sets of main-vernier pairs of the actuators, for example, for a motor and a PZT in a version of the pathlength control, for a voice coil and a PZT in hard drive head control, or in a motor-generator and a bypass tube in a high-voltage power supply [4].

ACKNOWLEDGEMENT

The research was carried out by the Jet Propulsion Laboratory, California Institute of Technology, under a contract with the National Aeronautic and Space Administration. The authors thank Drs. John Spanos, Greg Neat and David Bayard for helpful discussions.

REFERENCES

1. H. W. Bode, *Network Analysis and Feedback Amplifiers design*. Van Nostrand, New York, 1945.
2 B. J. Lurie, *Feedback Maximization. Artech House*, Dedham, MA, 1986.
3. B. J. Lurie and P. J. Enright, *Classical Feedback Control*, manuscript.
4. B. J. Lurie, J. Daegas. An Improved High-Voltage DC Regulator for a Radar and Communication Transmitter. "Proc. 18th Power Modulator Symposium", Hilton-Head, 1988.
5. J. T. Spanos and M. C. O'Neal. Nanometer level optical control of the JPL phase B testbed. ADPA/AIAA/ASME/SPIE Conf. on Active Materials and Adaptive Structures, 1992.
6. R. L. Grogan, G. H. Blackwood, and R. J. Calvet. Optical Delay Line Nanometer Level Pathlength Control Law Design For Space-Based Interferometry, 1998.